Journal of Experimental Botany, Vol. 63, No. 16, pp. 5967–5978, 2012
doi:10.1093/jxb/ers242
This paper is available online free of all access charges (see http://jxb.oxfordjournals.org/open_access.html for further details)

Journal of Experimental Botany
www.jxb.oxfordjournals.org

RESEARCH PAPER

Disrupting the bimolecular binding of the haem-binding protein 5 (AtHBP5) to haem oxygenase 1 (HY1) leads to oxidative stress in *Arabidopsis*

Hye-Jung Lee[1], Nobuyoshi Mochizuki[2], Tatsuru Masuda[3] and Thomas J. Buckhout[1,*]

[1] Applied Botany, Institute of Biology, Humboldt University Berlin, Invalidenstraße 42, 10115 Berlin, Germany
[2] Department of Botany, Graduate School of Science, Kyoto University, Kitashirakawa, Kyoto 606–8502, Japan
[3] Department of General Systems Studies, Graduate School of Arts and Sciences, University of Tokyo, Komaba 3-8-1, Tokyo, 153–8902, Japan

* To whom correspondence should be addressed: E-mail: h1131dqy@rz.hu-berlin.de

Received 26 May 2012; Revised 2 August 2012; Accepted 6 August 2012

Abstract

The *Arabidopsis thaliana* L. SOUL/haem-binding proteins, AtHBPs belong to a family of five members. The *Arabidopsis* cytosolic AtHBP1 (At1g17100) and AtHBP2 (At2g37970) have been shown to bind porphyrins and metalloporphyrins including haem. In contrast to the cytosolic localization of these haem-binding proteins, *AtHBP5* (At5g20140) encodes a protein with an N-terminal transit peptide that probably directs targeting to the chloroplast. In this report, it is shown that AtHBP5 binds haem and interacts with the haem oxygenase, HY1, in both yeast two-hybrid and BiFC assays. The expression of *HY1* is repressed in the *athbp5* T-DNA knockdown mutant and the accumulation of H_2O_2 is observed in *athbp5* seedlings that are treated with methyl jasmonate (MeJA), a ROS-producing stress hormone. In contrast, *AtHBP5* over-expressing plants show a decreased accumulation of H_2O_2 after MeJA treatment compared with the controls. It is proposed that the interaction between the HY1 and AtHBP5 proteins participate in an antioxidant pathway that might be mediated by reaction products of haem catabolism.

Key words: *Arabidopsis*, haem oxygenase, oxidative stress, haem-binding protein.

Introduction

Haem is prominent among the iron binding molecules in the cell. This tetrapyrrole binds ferrous iron (Fe^{2+}) at four co-ordinated nitrogens in the protoporphyrin ring system and is incorporated into many apo-proteins as a prosthetic group (Kumar and Bandyopadhyay, 2005). Free haem molecules can react with oxygen at one of the two uncoordinated binding sites of Fe^{2+}, producing Fe^{3+} and reactive oxygen species (ROS; Balla *et al*., 2003). The presence of free haem in the cytoplasm must be maintained at a low concentration (<0.1 μM) to prevent oxidative stress through the oxidation of haem iron (Khan and Quigley, 2011).

In higher plants, haem is synthesized by the tetrapyrrole biosynthesis pathway in plastids, sharing a common biosynthetic pathway with chlorophyll up to the intermediate protoporphyrin IX. At this point the pathway diverges into the Fe^{2+} and Mg^{2+} branches and continues with the ferro- or Mg-chelatase, respectively (Mochizuki *et al*., 2010). Haem is widely distributed in the cell; although, its allocation and trafficking into the cytosol, endoplasmic reticulum, mitochondria or other target organelles in plant cells are not well understood. The degradation of haem is mediated by haem oxygenase (HY or HO), a mixed function oxidase that catalyses the oxidative cleavage of the α methine carbon atom of haem, producing biliverdin-IXα (BV-IXα), Fe^{2+}, and CO (Khan and Quigley, 2011). In higher plants BV-IXα can be further reduced to phytochromobilin (PΦB), which serves as a chromophore for phytochrome (Terry *et al*., 2002). The phytochrome-deficient mutants *hy1*, *pcd1*, and *se5* in

Arabidopsis, pea (*Pisum sativum* L.), and rice (*Oryza sativa* L.), respectively, all lack haem oxygenase 1 and show an impaired conversion of haem to BV-IXα. Several haem oxygenase genes have been found in higher plants (Davis *et al*., 1999; Muramoto *et al*., 1999; Izawa *et al*., 2000). *Arabidopsis*, for example, has four *HO* genes, *HY1* (synonymous with *HO1*, At2g26670), *HO3* (At1g69720), and *HO4* (At1g58300) that belong to the HO-1 subfamily and encode putative haem oxygenases. *HO2* (At2g26550) is the sole member of the HO-2 subfamily and shows stable, high affinity binding to protoporphyrin IX *in vitro* (Gisk *et al*., 2010). The principal difference between the HO-1 and HO-2 subfamilies is a 15 amino acid insertion in HO-2 that is rich in aspartate and glutamate and the absence of a conserved histidine that is presumably necessary for haem binding (Davis *et al*., 2001). In *Arabidopsis* (Col-0), the transcription level of *HY1* is significantly higher than *HO2*, *HO3*, and *HO4* in most tissues. Phenotypic studies with the *ho1* single mutant and *ho* double or triple mutants demonstrate that the *hy1* null mutant dramatically alters plant growth and development, indicating its dominant function in photomorphogenesis (Emborg *et al*., 2006).

HO also participates in cell defence against oxidative stress in higher plants. It was reported that reactive oxygen species (ROS) triggered the expression of *HY1* in soybean and wheat plants (Noriega *et al*., 2004; Chen *et al*., 2009; Wu *et al*., 2011). Similarly, the cytoprotective signal, potentiated by low concentrations of nitric oxide (NO) under UV-B irradiation, was associated with the enhanced expression of *HO* (Yannarelli *et al*., 2006; Santa-Cruz *et al*., 2010). This response to oxidative stress was confirmed at the transcript, protein and enzyme activity levels.

Haem is relatively hydrophobic, and it is difficult to envisage how a product of a membrane-localized ferrochelatase would have access to the soluble stromal protein, HO (Joyard *et al*., 2009). Furthermore, since the products of HO, Fe^{2+}, CO, and BV-IXα, are themselves reactive catabolites, it is essential that haem metabolism be regulated. We speculate that the transfer of haem to HO requires a carrier protein.

AtHBP2 was initially identified as a phytochrome A-induced transcript that rapidly responded to light during de-etiolation (Khanna *et al*., 2006). *AtHBP2* encodes a p22HBP/SOUL protein and belongs to a family of six *Arabidopsis* genes. The amino acid sequences of the AtHBPs are homologous to mammalian SOUL and p22HBP (*haem-b*inding *p*rotein), which were initially purified from vertebrates and have been shown to bind cytosolic haem (Taketani *et al*., 1998; Zylka and Reppert 1999). These vertebrate haem-binding proteins were considered to function in transfer or delivery mechanisms of cytosolic haem to apoproteins (Jacob Blackmon *et al*., 2002; Babusiak *et al*., 2005; Dias *et al*., 2006). Takahashi *et al*. (2008) have shown that cytosolic *Arabidopsis* AtHBP1 (At1g17100) and AtHBP2 (At2g37970) bound porphyrins, including haem, and they proposed that these two HBPs were cytosolic tetrapyrrole-carrier proteins.

In contrast with the putative cytosolic AtHBPs, AtHBP3 and AtHBP5 (At3g10130 and At5g20140, respectively) have N-terminal transit peptides that are predicted to target chloroplasts. However, haem binding by these proteins has not been shown. In the present report, the physiological function of AtHBP5 was characterized by genetic and biochemical methods and by mutant analysis. Our data show that AtHBP5 is a haem-binding protein that interacts with the haem oxygenase 1 (HY1) in chloroplasts and that *HY1* expression is repressed in an *athbp5* knockdown mutant. It is proposed that the bimolecular binding of AtHBP5 and HY1 participates in an antioxidant pathway presumably through an influence on haem catabolism.

Materials and methods

Plant material, transformation methods and growth conditions

Arabidopsis thaliana (L.) Heynh. (Columbia-0) was used for all the experiments. The T-DNA insertion line for the *AtHBP5* gene, sail_1280_C03, was obtained from NASC (Nottingham, UK). To generate *AtHBP5* over-expressing plants, full-length *AtHBP5* from cDNA was placed under the control of the cauliflower mosaic virus 35S-promoter and introduced into wild-type *Arabidopsis* plants by the floral dip method using *Agrobacterium*-mediated transformation (Clough and Bent, 1998). The genotypes of the T-DNA mutant were confirmed using PCR analysis, and immunoblots were usd to identify over-expressing transgenic plants using a polyclonal anti-AtHBP5 antibody (see below). Plants were grown on ES agar medium (Gollhofer *et al*., 2011) at 21 °C under a 10 h light (95 μmol m^{-2} s^{-1}) /14 h dark photoperiod or on soil as indicated.

Construction of AtHBP *expression plasmids and recombinant protein expression in* E. coli

The sequences encoding full-length *AtHBP1, 2, 3*, and *5* were amplified from *Arabidopsis* cDNA with the primers shown in Supplementary Table S1 at *JXB* online. The amplified fragments were cloned into the pGEM-T vector (Promega), and constructs were confirmed by sequencing (SMB GmbH, Berlin, Germany). The fragments were digested with *Nde*I/*Sal*I to yield *AtHBP1*, *AtHBP2*, and *AtHBP3* or *Nhe*I/*Xho*I to yield *AtHBP5*, and then cloned into pET-24a or pET-28a vectors (Merck Chemicals). The expression vectors containing the *AtHBP* genes fused to a 6xHis tag, were introduced into *E. coli* [BL21(DE3) or C43(DE3)]. Expression of the 6xHis tagged recombinant proteins was induced at 20 °C by adding isopropyl-β-D-thiogalactopyranoside (IPTG) to a final concentration of 0.05 mM. Recombinant proteins were purified using Ni^{2+}-NTA agarose (Qiagen) under native conditions.

The coding sequence for the mature AtHBP5 protein excluding the N-terminal 52 amino acids was amplified with the appropriate primers (see Supplementary Table S1 at *JXB* online), and the fragment cloned into the pGEM-T. After validation of the amplified nucleotide sequence, the fragment was inserted into pET-24(+) and transformed into *E. coli* BL21 (DE3). Synthesis of the 6xHis-tagged mature AtHBP5 protein was induced at 30 °C by the addition of IPTG to a final concentration of 0.2 mM, and the recombinant protein was purified using an IMAC cartridge (Bio-Rad) under denaturing conditions. The purified AtHBP5 protein was used as an antigen for production of the anti-AtHBP5 antibodies (Operon, Japan).

Haem binding assay

Haem binding was performed followed the method of Mills and Payne (1995). Briefly, the proteins AtHBP1, AtHBP2, AtHBP3, and AtHBP5 were diluted in resuspension buffer (20 mM TRIS-HCl, pH 8.0, 150 mM NaCl) and incubated with 50 μl of pre-equilibrated hemin agarose (H6390, Sigma-Aldrich; packed volume, >4 μmol ml^{-1}) for 0.5 h at room temperature on a rotary shaker. The mixture was centrifuged for 5 min at 750 *g* and the pellet washed three times with high-salt buffer (20 mM TRIS-HCl, pH 8.0, 20 mM EDTA and 1 M NaCl) to remove non-specifically bound proteins. The resin mixture was washed once in an equilibration solution, and finally suspended in 100 μl SDS sample buffer. The hemin-bound protein was subjected to SDS-PAGE analysis, followed by immunoblotting and detection with horseradish peroxidase (HRP)-conjugated anti-His antibody (Sigma-Aldrich).

Screening for protein-protein interactions by yeast two-hybrid analysis

The coding regions of *AtHBP1, AtHBP2, AtHBP3, AtHBP5*, and *HY1* (At2g26670) were amplified without the predicted signal peptide from *Arabidopsis* cDNA with the appropriate primers (see Supplementary Table S1 at *JXB* online) by PCR. The amplified fragments were cloned into the TA-cloning vector and sequenced. The fragments were digested and subcloned into pBTM117c vector that contained the LexA DNA-binding and into pGAD10 that contained the GAL4 activation domain (Wanker *et al*. 1997). These vectors were used for yeast two-hybridization. *Saccharomyces cerevisiae* strain L40ccua was co-transformed with bait and prey vectors by the lithium acetate method, and the positive transformants were verified by growing on selection medium (SC-trp-leu). For interaction screening, yeast transformants were grown on SC-trp-leu-his-ura medium, and β-galactosidase activity was assayed using the X-gal filter lift method. The actively growing colonies were blotted onto nitrocellulose filters. The filters were frozen in liquid nitrogen, thawed at room temperature for 30 s, and placed on Whatman 3MM paper saturated with X-gal solution for detection of β-galactosidase activity.

Split yellow fluorescence protein (YFP) for protein interaction analysis

For the *in vivo* protein interaction, the bimolecular fluorescence complementation (BiFC) method described by Walter *et al*. (2004) was adapted. The modified YFP split binary vectors, pSPY*N*E-35S/pUC-SPY*N*E, which encodes the *N*-terminal fragment of YFP, and pSPY*C*E-35S/pUC-SPY*C*E, encoding the *C*-terminal fragment of YFP both under the control of the 35S promoter, were used. The open reading frames of *AtHBP5* and *HY1* were cloned using the appropriate primers (see Supplementary Table S1 at *JXB* online) and verified by sequencing. In parallel, cloning of *HY1* and *AtHBP5* genes without the predicted N-terminal transit peptide was also conducted using the primers listed in Supplementary Table S1 at *JXB* online. The amplified fragments were digested with *Sma*I and subcloned into the corresponding binary vectors. The combinations of *AtHBP5*_YFP^c and *HY1*_YFP^n or *AtHBP5*_YFP^n and *HY1*_YFP^c BiFC binary vectors were transiently expressed in tobacco (*Nicotiana benthamiana*) leaves. Three days after transformation, the infiltrated tobacco leaves were observed under a confocal laser scanning microscope (TCS SP2, Leica).

Identification of T-DNA mutant and semi-quantitative reverse transcriptase (RT)-PCR analysis

The *AtHBP5* T-DNA insertion mutant was initially grown on soil and selected for herbicide resistance by spraying with BASTA (0.01%). The mutants surviving the herbicide treatment were screened by PCR genotyping using gene-specific primers (see Supplementary Table S1 at *JXB* online). Total RNA was extracted from T-DNA mutant plants using TRIsure (Bioline), and 1 μg RNA was treated for 30 min with Dnase I as described in the Fermentas manual. cDNA was synthesized using Revert Aid M-MuLV Reverse Transcriptase (Fermentas). Semi-quantitative PCR was used for the analysis of gene expression and PCR primers were designed with PerlPrimer software (see Supplementary Table S1 at *JXB* online; Marshall, 2004).

Plant treatment and detection of H_2O_2

Arabidopsis seeds were surface-sterilized for 3 min with 4% (v/v) NaOCl and rinsed five times with sterile dH_2O. Seeds were planted on ES-agar and vernalized for 5 d at 4 °C in the dark. One week-old *athbp5*, *AtHBP5* over-expressing transformants, and wild-type seedlings were treated with 200 μM MeJA by spraying and incubated for 3 d.

Diaminobenzidine (0.1% DAB) solutions (D4168, Sigma-Aldrich) were prepared in dH_2O. The MeJA-treated seedlings were incubated in the DAB solution at room temperature in the dark until brown spots appeared. The reaction was stopped by immersion of the seedlings in boiling ethanol (96%) for 10 min and the DAB-stained seedlings were photographed. Determination of H_2O_2 in plant tissues was conducted using the method of Zhou *et al*. (2006). Briefly, 0.3 g of MeJA-treated seedlings was ground in liquid N_2 to which 3 ml of 5% TCA and 0.1 g activated charcoal (Sigma-Aldrich) were added. The homogenate was cleared by centrifugation, and the pH of the extract was adjusted to 8.4 with ammonia hydroxide. The filtered extract was divided into aliquots of 1 ml. Catalase was added to one aliquot, which was subsequently used as a blank. The H_2O_2 content in the remaining aliquots was determined colorimetrically at 505 nm.

Determination of haem, chlorophyll and carotenoid

The haem content of intact plants was determined by the chemiluminescence of HRP using the method of Espinas *et al*. (2012). Chlorophyll and carotenoid content were determined according to Melis *et al*. (1987) and according to Lichtenthaler (1987), respectively.

Results

Phylogenetic analysis of SOUL/haem-binding proteins (HBPs)

In a search of the NCBI (National Center for Biotechnology Information) database for plant genes containing a SOUL/*haem-b*inding *p*rotein (HBP) domain, 62 proteins from flowering plants, a conifer, and a club-moss were found. These were subjected to a phylogenetic analysis (see Supplementary Fig. S1 at *JXB* online). Five *Arabidopsis* p22HBP/SOUL proteins were found in both *A. thaliana* and *A. lyrata*, and in two subspecies of rice (*O. sativa* Japonica and Indica groups). An additional gene locus in *Arabidopsis*, At1g78450, which showed high sequence similarity to SOUL/HBPs, has been identified as a pseudogene (Takahashi *et al*., 2008) and was therefore not included in the analysis. An unrooted, radial phylogenetic tree of higher plant p22HBP/SOUL amino acid sequences was constructed using the Neighbor–Joining method, and the reliability of the phylogenetic tree was confirmed using a bootstrap re-sampling strategy (Tamura *et al*., 2011). The resulting tree was divided into five clearly distinct clades, of which four contained at least one *Arabidopsis* p22HBP/SOUL (see Supplementary Fig. S1 at *JXB* online). Interestingly, *Arabidopsis* sequences were not found in clade 4, which, however, contained representatives of all other genera analysed (see Supplementary Fig. S1 at *JXB* online). Clade 2 included nine sequences from flowering plants but lacked sequences from *Picea* und *Selaginella* (see Supplementary Fig. S1 at *JXB* online). The members of clades 1, 2, 3, and 4 formed a clade of clades, whereas clade 5 displayed a sister group-like relationship among members.

The recombinant proteins AtHBP1*,* AtHBP2*, and* AtHBP5 *bind haem* in vitro

The haem binding activity of the putative AtHBPs was initially investigated. The full-length *AtHBP1, AtHBP2, AtHBP3*, and *AtHBP5* coding sequences were cloned from wild-type *Arabidopsis* cDNA and expressed in *E. coli*. Although most His-tagged recombinant AtHBPs were present in inclusion bodies from the bacterial cells, it was possible to express the soluble AtHBPs under non-denaturing conditions by growing cells

at 20 °C. Recombinant AtHBPs were detected using an anti-His tag antibody after separation by SDS-PAGE. For binding assays using a batch procedure, pre-equilibrated hemin-agarose was added to the purified recombinant AtHBPs and non-hemin-bound proteins were subsequently removed by washing with a high salt buffer. Bound AtHBPs were eluted with SDS sample buffer, separated by SDS-PAGE (12% acrylamide), blotted onto a PVDF membrane, and immunologically detected.

Using this procedure, the recombinant AtHBP5 protein was detected in the fraction bound to hemin-agarose (Fig. 1A, lane 'HA'). Binding of AtHBP1 and AtHBP2 to hemin-agarose was also observed (Fig. 1A, lane 'HA'), confirming the previous observation of Takahashi *et al*. (2008). The His-tag antibody recognized the recombinant AtHBP3 protein in the second high-salt wash fraction ('HS2'), but no signal was detected in the bound fraction (Fig. 1A, lane 'HA'). Thus, it was concluded that the AtHBP5 bound to hemin-agarose, while the binding of AtHBP3 was non-specific.

To verify the specificity of the haem-AtHBP5 protein complex, the absorbance spectrum of haem upon addition of the purified AtHBP5 protein was monitored. The recombinant AtHBP5 protein, lacking the predicted signal peptide, was cloned and expressed in *E. coli*. The AtHBP5 protein was resuspended in TRIS buffer (20 mM TRIS-HCl, pH 6.5), incubated with 5-fold excess of hemin for 20 min on ice, and the spectrum analysed. Upon addition of the AtHBP5 protein, the broad Soret band of free hemin was intensified and λ_{max} shifted from 398 nm to 413 nm. In addition, Q-bands appeared around 540 nm (Fig. 1B). This shift was attributed to the co-ordination of hemin by the AtHBP5 protein. A similar spectral shift in the Soret region has been previously observed for the Fe^{3+}-haem–SOUL complex (Sato *et al*., 2004). When the reaction was performed at pH 2.2, the peak in the Soret region was widened but λ_{max} was largely unchanged (Fig. 1B). These data supported haem binding by AtHBP5.

Protein–protein interaction between AtHBP5 and HY1

The AtHBP5 protein had an N-terminal extension, which was not found in AtHBP1, AtHBP2 or mammalian homologues. AtHBP5

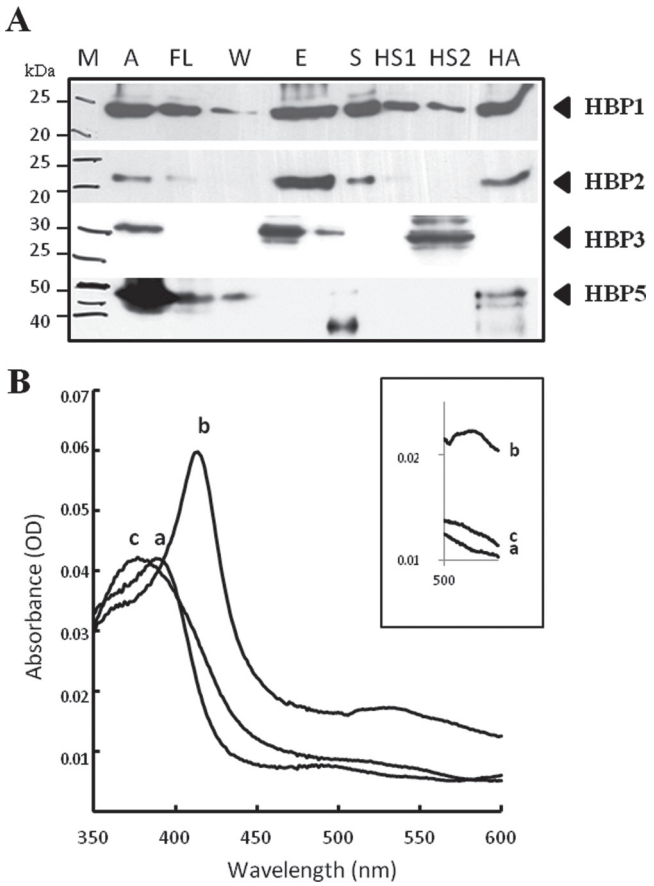

Fig. 1. (A) Haem-binding activity of recombinant AtHBPs. Total protein extracts from *E. coli* following IPTG treatment (fraction 'A') were chromatographed on a Ni^{2+}-agarose column. The column was washed with loading buffer and eluted with imidazole buffer ('FL'=flow-through fraction, 'W' and 'E'=wash and eluted fractions, respectively). The eluted fractions were concentrated and bound in a batch method to hemin-agarose beads. The beads were washed twice with high-salt-containing buffer and eluted with SDS sample buffer. 'S' is the soluble fraction after incubation with hemin-agarose beads, 'HS1' and 2 are high-salt wash fractions, 'HA' the eluted HBP fraction, and M is the molecular mass marker. (B) Spectrophotometric analysis of haem binding to AtHBP5. The purified AtHBP5 protein was incubated with a 5-fold excess of hemin for 20 min on ice and the spectrum analysed (b). The spectrum of hemin alone (a) or hemin plus AtHBP5 at pH 2.2 (c) are also shown.

was predicted to be localized in chloroplasts (Emanuelsson *et al*., 2007) and was identified in chloroplasts by mass spectrometry (Zybailov *et al*., 2008). As HY1 is a crucial enzyme in haem homeostasis, the possibility was considered that AtHBP5 might be involved in the delivery of haem to HY1 in chloroplasts.

The protein–protein interaction between AtHBP5 and HY1 was examined in a yeast two-hybrid system. The bait or prey plasmids containing *HY1* and *AtHBPs* were co-transformed into an L40ccua yeast strain as described (see Materials and methods). The co-transformed yeast cells were tested for the activation of the *LacZ* reporter gene, as well as for growth on media lacking tryptophan, leucine, histidine, and uracil. After 24 h incubation, the X-gal product was visible only in yeast cells co-expressing HY1 and AtHBP5 fusion proteins. The activity of the reporter gene was silent in the other yeast colonies (Fig. 2A). Similar results were obtained when the bait and prey vectors were reversed. Thus, the results of the yeast two-hybrid analysis supported a protein–protein interaction between HY1 and AtHBP5.

To verify the interaction of HY1 and AtHBP5 in living plant cells, a bimolecular fluorescence complementation (BiFC) assay was used. YFP sequences encoding either the N-terminal 155 amino acids or the C-terminal 86 amino acids were fused to the full-length *HY1* or *AtHBP5* genes (*AtHBP5*-YFP^c and *HY1*-YFP^n or *AtHBP5*-YFP^n and *HY1*-YFP^c). Tobacco leaves were transiently co-transformed and yellow fluorescence was observed using an excitation wavelength from 490–510 nm. In leaves that co-expressed with *AtHBP5*-YFP^c and *HY1*-YFP^n, a yellow fluorescent signal co-localized with the red autofluorescence of chlorophyll (Fig. 2B). Tobacco leaves transformed with any combination of empty binary vectors showed chlorophyll fluorescence but no YFP signal (Fig. 2C). These results confirmed a protein–protein interaction between HY1 and AtHBP5 in chloroplasts.

A fluorescence signal could not be detected in leaves co-expressing C-terminal YFP-HY1 and N-terminal YFP-AtHBP5 fusion proteins (*AtHBP5*-YFP^n and *HY1*-YFP^c). It was speculated that this lack of signal was caused either by the

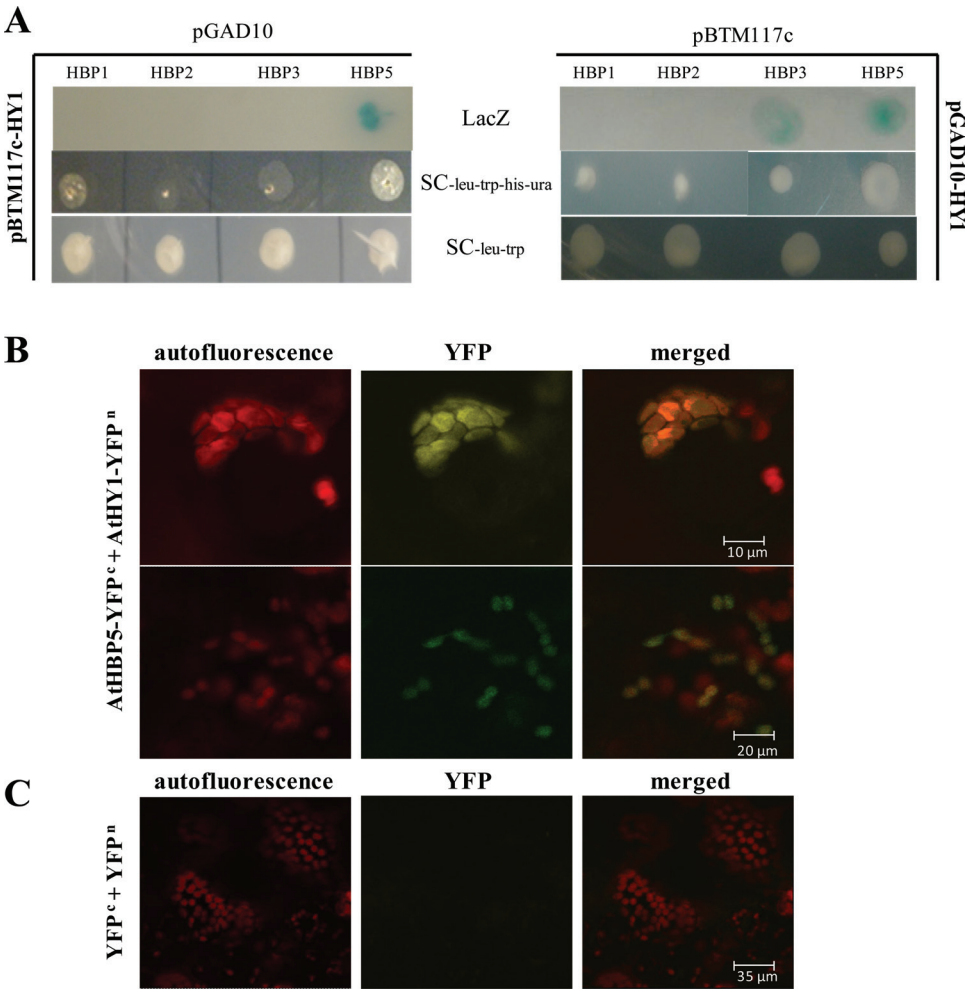

Fig. 2. Demonstration of a protein–protein interaction between HY1 and AtHBP5 by yeast-two-hybrid (A) and BiFC (B) assays. (A) Shown are results of the two-hybrid assay using HY1 as bait and the HBPs as prey and vice versa. SC, selection medium lacking leu, trp, his, and uracil (ura) as indicated. LacZ is the activity of a reporter gene encoding β-galactosidase. (B) A BiFC assay showing co-expressed of HY1 fused at the N-terminus and AtHBP5 at the C-terminus to split YFP. (C) Results from a BiFC analysis in cells transformed with empty binary vectors. The YFP fluorescence is displayed as yellow or green colours for a more distinct merged signal.

incorrect refolding of the YFP fusion protein or by rapid turnover of the complex. On the other hand, when the BiFC experiment was conducted with HY1 and AtHBP5 proteins that lacked the 50 and 52 N-terminal amino acid sequences, respectively, the YFP-derived fluorescence signal was visible in the cytoplasm of the tobacco epidermal cells but not in plastids (see Supplementary Fig. S2 at *JXB* online). These results confirm the interaction of HY1 with AtHBP5.

Characterization of an athbp5 *T-DNA mutant*

To clarify the physiological function of AtHBP5 further, a T-DNA mutant with an insert in the 3rd intron of *AtHBP5* was obtained, and five homozygous lines were selected by PCR screening. No amplification product was observed with endogenous primers in homozygous *athbp5* T-DNA lines (Fig. 3A, left panel). The *AtHBP5* transcript in the T-DNA mutants was investigated using semi-quantitative RT-PCR analysis with gene-specific primers. PCR products corresponding to the *AtHBP5* gene were observed with template cDNA from the wild type and a heterozygous (*athbp5 11–2*) but not in homozygous *athbp5* lines, indicating that the *AtHBP5* transcript was greatly reduced in the homozygous T-DNA mutant.

To address the transcriptional activity of *HY1* in the *athbp5* T-DNA mutant, semi-quantitative-PCR analysis was conducted using *HY1* gene-specific primers in wild-type, heterozygous, and homozygous *athbp5* plants. As shown in Fig. 3A (right panel), the expression of *HY1* was decreased in the *athbp5* lines, whereas the heterozygous T-DNA mutant, *athbp5_11-2*, showed no apparent difference in expression of *HY1* when compared with the wild-type plants. Down-regulation was not observed for *HO3* in all cases investigated. These data indicated that the

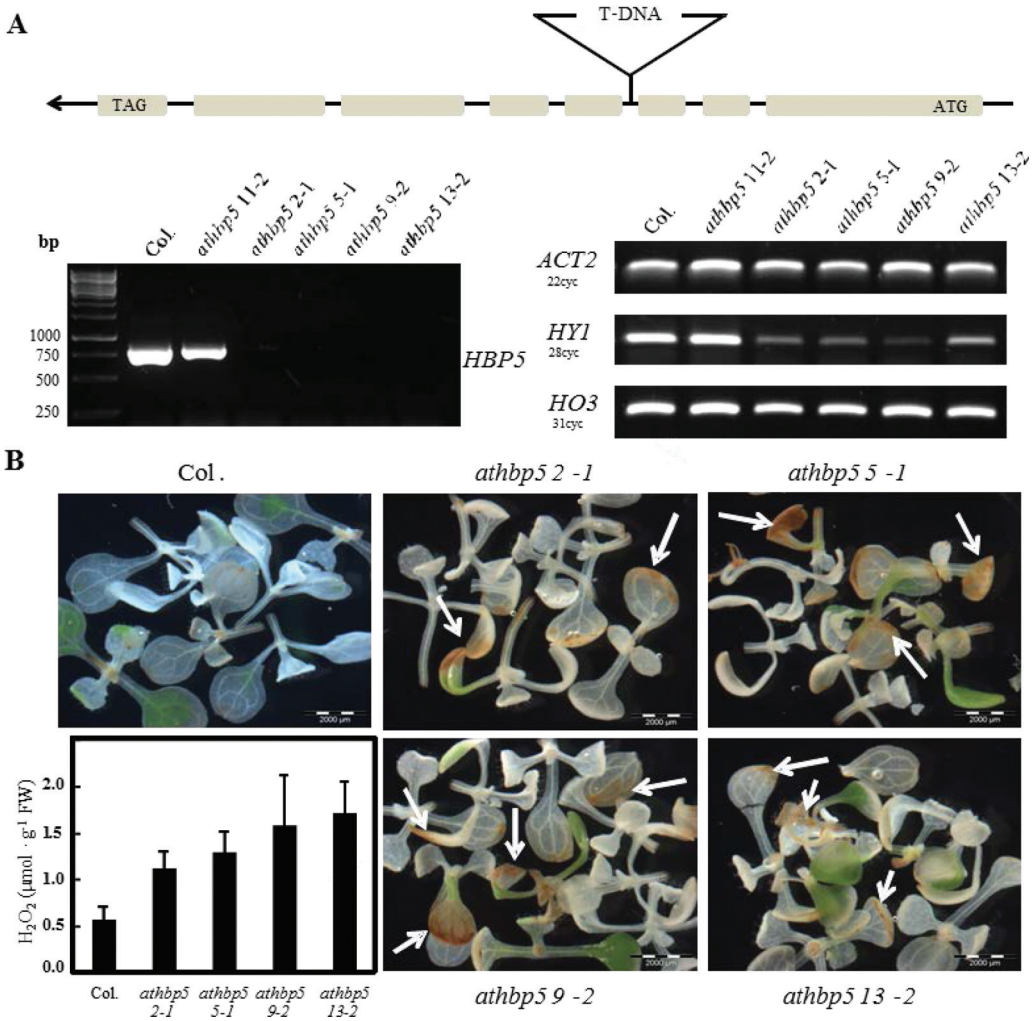

Fig. 3. Genotyping PCR and RT-PCR analysis of the *athbp5* mutant and the response of this mutant to oxidative stress. (A) The top panel illustrates the location of the T-DNA insertion in the *AtHBP5* gene. The bottom-left panel shows the results of a PCR analysis on genomic DNA. Signals for *AtHBP5* were observed only in the wild-type and the *athbp5 11–2* heterozygous line. No PCR product was observed in the homozygous lines. The lower-right PCR gel shows the results of a semi-quantitative RT-PCR using *AtACT2* as a standard. *ACT2*=At3g18780, *HY1*=At2g26670, and *HO3*=At1g69720. (B) Seven-day-old *Arabidopsis* seedlings were treated with 200 μM MeJA to induce oxidative stress. The seedlings were stained in DAB buffer for 16 h in darkness. The presence of H_2O_2 is indicated by brown-coloured staining of the leaves (arrows). The quantitative analysis of H_2O_2 is also shown in (B) (lower left).

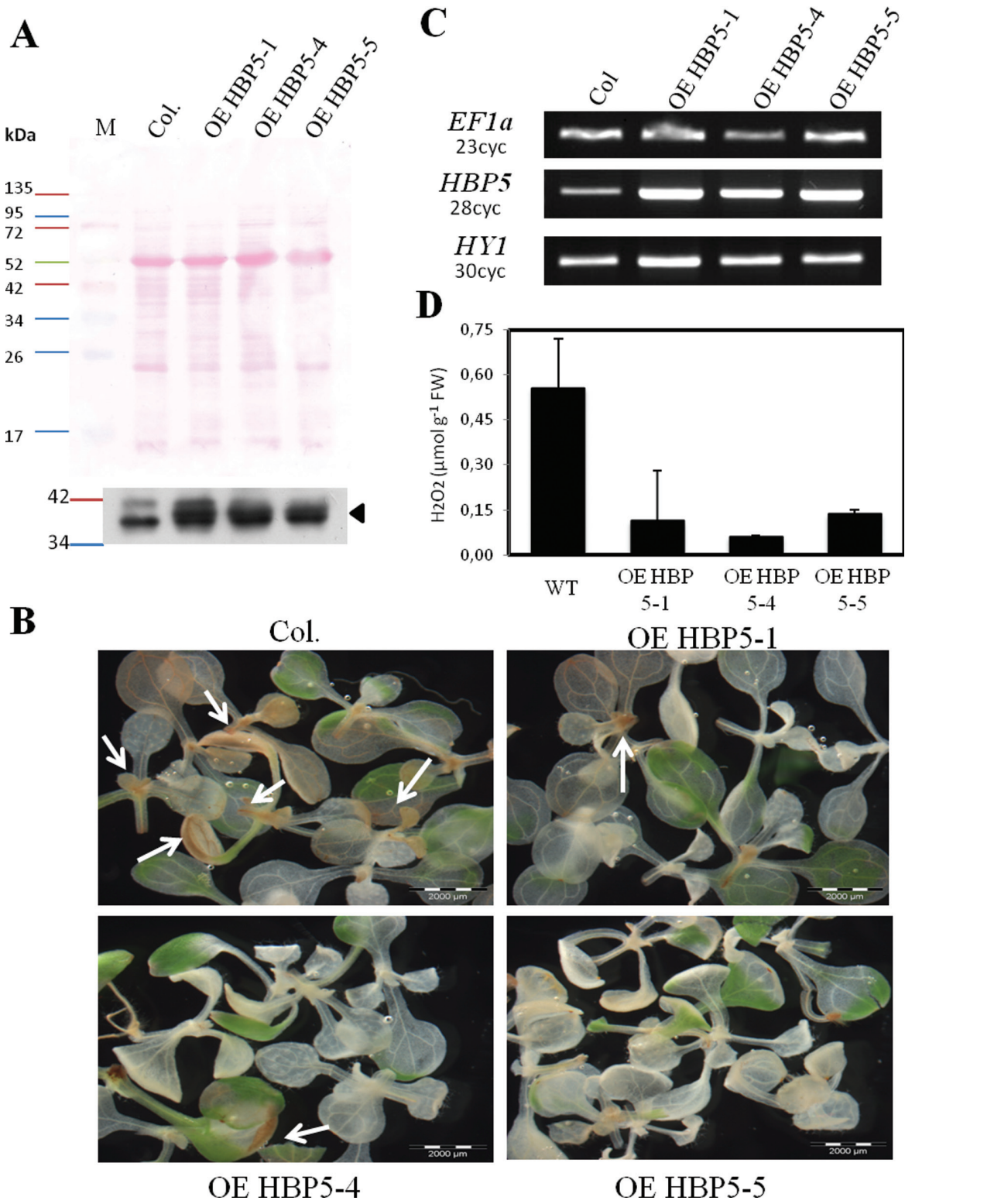

Fig. 4. Analysis of *AtHBP5* over-expressing transgenic plants using an anti-AtHBP5 antibody and the response of OE plants to oxidative stress. (A) The transgenic *Arabidopsis* plants were transformed with full-length *AtHBP5* under the control of a 35S promoter. Fifteen µg of total protein were loaded per lane, and the protein expression level of AtHBP5 in leaves was analysed using rabbit anti-AtHBP5 antiserum (lower panel). The mature AtHBP5 protein was detected at the predicted molecular mass of 37.2 kDa. A Ponceau-stained membrane is shown as a loading control. (B) Seven-day-old *Arabidopsis* seedlings were treated with 200 µM MeJA to induce oxidative stress. The seedlings were stained in DAB buffer for 21 h in darkness. The presence of H_2O_2 is indicated by brown-coloured staining of the leaves (arrows). (C) Quantification of *AtHBP5* and *HY1* transcription by semi-quantitative RT-PCR on untreated *AtHBP5* over-expressing transgenic plants. Description of genes: *EF1*α=At5g60390, *AtHBP5*=At5g20140, and *HY1*=At2g26670. (D) Quantitative analysis of the H_2O_2 concentration in the over-expression *AtHBP5* lines.

transcript level of *HY1* is specifically down-regulated in the absence of *AtHBP5* and might have resulted in decreased haem oxygenase activity.

Accumulation of H_2O_2 in the athbp5 *T-DNA mutant treated with MeJA*

Haem oxygenase1-deficient, murine embryonic fibroblasts (MEFs) had notably increased free radical production when the fibroblasts were cultured in the presence of the oxidants, hemin and H_2O_2 (Poss and Tonegawa, 1997). These data together with results of others (True *et al*., 2007) indicated a potentially important antioxidant function for haem oxygenase, particularly under conditions of oxidative stress. To understand the effect of repressed *HY1* expression in *athbp5* mutant plants, the mutants and the wild-type were treated with methyljasmonate (MeJA) which, when applied in excess, induced cell death through the accumulation of ROS (Zhang and Xing, 2008). H_2O_2 was detected by DAB staining. In the mutant leaves, H_2O_2 production was apparent as brown-colored staining on the leaf margins, while in wild-type seedlings little or no leaf staining was observed (Fig. 3B). The direct measurement of H_2O_2 confirmed the results of DAB staining. The H_2O_2 concentration was increased between 2- and 3-fold in the T-DNA mutant. These data indicated that the T-DNA insertion mutant showed enhanced susceptibility to oxidative stress, which might have been caused by loss of ROS detoxification activity in the mutant.

AtHBP5 *over-expression enhanced antioxidant resistance under oxidative stress*

The accumulation of H_2O_2 was observed in the *athbp5* mutant following treatment with MeJA. This result indicated that the ROS concentration in the cell was altered when *AtHBP5* or *HY1* expression was compromised. To verify the transcriptional regulation of *HY1* by AtHBP5, *AtHBP5* over-expressing (OE HBP5) transgenic plants were constructed. The increased concentration of AtHBP5 protein was demonstrated by a Western blot using an anti-AtHBP5 antibody. The mature AtHBP5 protein was detected at the predicted molecular mass (37.2 kDa) in both wild-type and OE HBP5 transgenic lines (Fig. 4A, lower panel). We observed an increased AtHBP5 protein in over-expressing lines compared with the wild-type.

One-week-old seedlings of OE HBP5 transgenic lines were subjected to MeJA treatment. As shown in Fig. 4B, the brown staining on the leaf margins was only faintly visible in the over-expressing lines, whereas brown staining was extensive in the wild-type plants. Direct measurement showed an 80–90% decrease in H_2O_2 in the over-expressing plants (Fig. 4D). As predicted, over-expression of AtHBP5 resulted in plants that were less sensitive to MeJA treatment compared with the T-DNA mutant. Thus, the over-expression of AtHBP5 protein increased the ROS scavenging activity. To examine whether the over-expression may consequently modulate the transcriptional activity of *HY1*, an analysis of transcript abundance was conducted on the OE HBP5 plants (Fig. 4C). Consistent with the over-expression of AtHBP5 (Fig. 4A, lower panel), the transcription level of *AtHBP5* was increased in the OE HBP5 transgenic lines. It was also observed that the transcription of *HY1* was slightly increased compared with that of the wild-type. Considering the striking decrease of mRNA expression of *HY1* in the *athbp5* mutant, this difference may not be significant, but it is important to note that the over-expression of *AtHBP5* had an impact on the accumulation of ROS in cells.

Analysis of haem and photosynthetic pigments

Finally, the haem and pigment contents in the mutant and over-expressing lines were investigated. Whereas the chlorophyll and carotenoid concentration and the chlorophyll *a/b* ratio in the mutant and over-expressing lines were unaltered, the haem content was increased in the *athbp5* mutant but not in the over-expression lines. Mutation of *AtHBP5* resulted in a 25% increase in haem content in mutant plants (Fig. 5). Thus, it is plausible that the higher accumulation of H_2O_2 in the *athbp5* mutant was caused by an accumulation of haem and/or a decrease in haem catabolites.

Discussion

Despite the clear distinction between SOUL proteins and p22HBP in mammals, this distinction was not readily apparent in plants because of the lack of a conserved His residue and the absence of the distinct expression profiles of *Arabidopsis* AtHBPs. Therefore, all of the p22HBP/SOUL homologues in *Arabidopsis* have simply been referred to as haem-binding proteins (HBPs). In this report, the haem-binding ability of AtHBP5 has been demonstrated, and the results of Takahashi *et al*. (2008) have been confirmed for AtHBP1 and 2.

A phylogenetic analysis in plants grouped the HBPs into five clades based on sequence homology. Sequences in clades 1 and 2 are predicted to be localized in chloroplasts. AtHBP5 is located in clade 1 and its localization in chloroplasts supported experimentally (Fig. 2). Localization was assigned to secretory pathways for the sequences in clade 5, and no prediction could be made for the sequences in clade 3. All the sequences clustering in clade 1, including AtHBP5, contained an N-terminal NTF2-like domain, belonging to the nuclear transport factor2-like (NTF2-like) superfamily (see Supplementary Fig. S1B at *JXB* online). The NTF2-like domain was found in numerous proteins with widely divergent cellular functions (Dóczi *et al*., 2007), but the functional significance of this structure in HBPs is not known.

In this report, AtHBP5 has been identified as another member of the haem-binding protein family (Fig. 1A, 1B), whereas AtHBP3 was unable to bind to the hemin-agarose affinity column. Thus, these two proteins are not likely to have redundant functions in the cells. As a novel haem-binding protein, AtHBP5 is located in the chloroplast. A protein–protein interaction between HY1 and AtHBP5 (Fig. 2A) was demonstrated experimentally and, further, it was shown that, depending on the presence of chloroplast signal sequences, this interaction occurred in chloroplasts (Fig. 2B) or in the cytoplasm (see Supplementary Fig. S2 at *JXB* online).

Haem is produced from protoporphyin IX and Fe^{2+} by ferrochelatase, located in thylakoid and chloroplast envelope

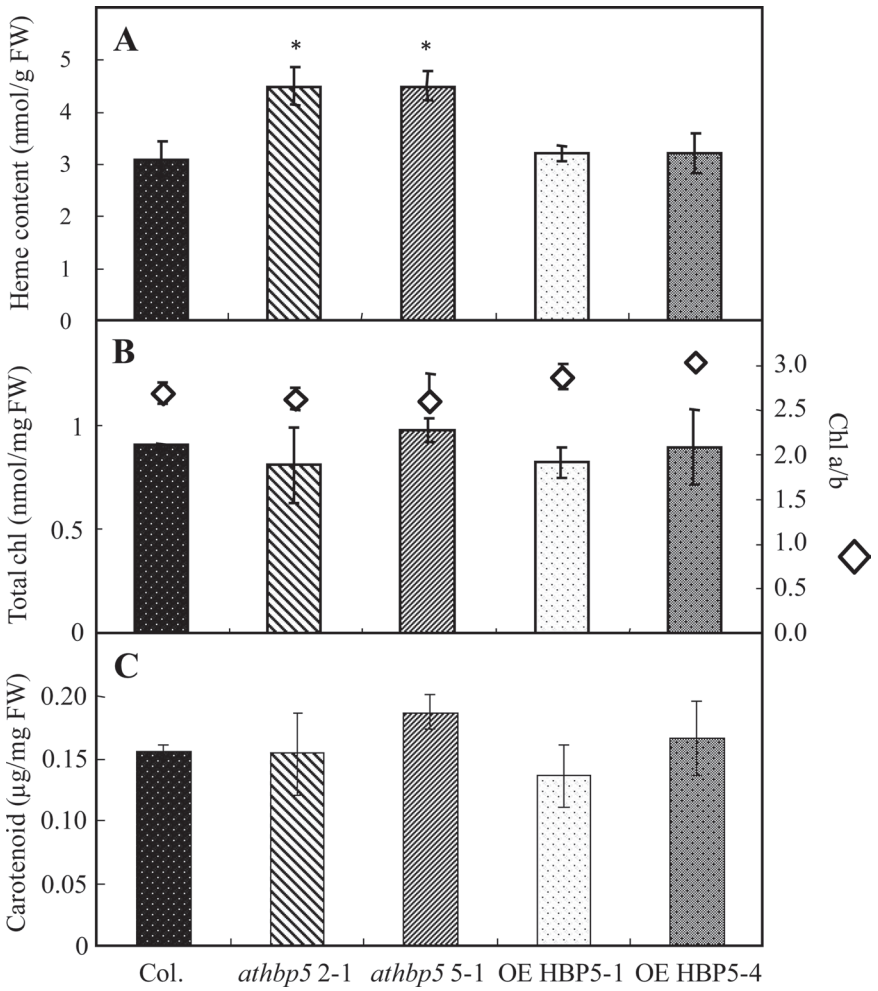

Fig. 5. An analysis of haem (A), chlorophyll (B) and carotenoid (C) content in *Arabidopsis* wild-type (Col.), *athbp5* T-DNA mutant and *AtHBP5* over-expressing transformants. Error bars indicate the standard error of the mean and asterisks indicted statistical differences from the Col. control at $P < 0.01$.

membranes (Roper and Smith, 1997). The product of ferrochelatase is released either within the chloroplast or exported to the cytoplasm. In the former case, haem would serve as a substrate for the haem oxygenase. Our data showing the formation of an AtHBP5–HY1 complex indicate a link between the membrane-bound protein ferrochelatase and the stomal enzyme HO. The substrate binding mechanisms, based on published protein structures, indicate that AtHBP5 may form a hydrophobic pocket with relatively high binding affinity for haem (K_d ~21 pM; Sato *et al*., 2004). By contrast, HY1 is believed to employ a His residue to co-ordinate ligand binding (K_d ~1.6 μM; Gisk *et al*., 2010). The haem binding to AtHBP5 could buffer the free haem at a low concentration and efficiently deliver haem to HY1.

In transcriptional analyses, *HY1* transcript abundance was decreased in the *athbp5* T-DNA mutant (Fig. 3A). Regardless of the decreased *HY1* mRNA abundance in *athbp5* plants, the mutant did not phenotypically copy the *hy1* mutant, and elongation of hypocotyls that were grown in the dark, red, far-red or blue light was not different from the wild-type (see Supplementary Fig. S3 at *JXB* online). The fact that the *athbp5* mutant did not phenocopy *hy1* was not likely due to multiple isoforms of the haem oxygenase. *HY1* expression was greatly decreased but not eliminated in the *athbp5* mutant (Fig. 3A). Perhaps this relatively low level of expression was sufficient to ameliorate the *athbp5* phenotype. On the other hand, haem accumulation as a result of decreased transcriptional activity of *AtHBP5* and *HY1* might have acted as a feedback inhibitor of glutamyl-tRNA reductase, which is the critical step in the regulation of tetrapyrrole biosynthesis.

The transcriptional co-expression of *HY1* was observed in both the *athbp5* mutant and in the over-expression lines. The signal pathway for this co-regulation remains enigmatic. A widespread co-expression of *AtHBP5* and *HY1* is not supported by published transcriptome analyses (e.g. Genvestigator, data not shown). This is perhaps not surprising, since the phenotype of the *athbp5* mutant does not overlap with that of *hy1* (=*gun2*). A possible mechanism for the repression of *HY1* in *athbp5* could be similar to the transcription factor-mediated *HO-1* regulation by Bach1-Maf dimer formation found in mammals; however, at present, we have no supporting evidence for such a mechanism (reviewed by Gozzelino *et al*., 2010).

The *athbp5* mutant showed significantly higher production of H_2O_2 compared with the wild-type following MeJA treatment

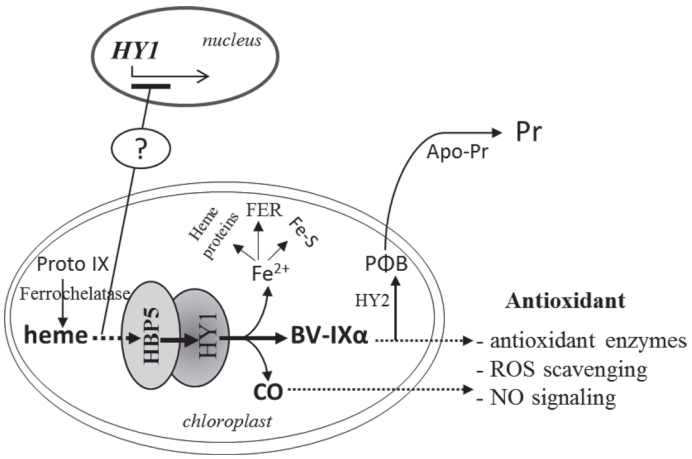

Fig. 6. Model depicting the binding of AtHBP5 and HY1 and proposed down-stream reaction leading to increased resistance to oxidative stress. In the absence of AtHBP5, the expression of HY1 is repressed by an unknown mechanism leading to the accumulation of haem and presumable to a decrease in haem breakdown products. The resulting reduction in the haem catabolites, BV-IXα and CO, would render the plants more susceptible to oxidative stress resulting from MeJA treatment.

(Fig. 3B). Reduced *AtHBP5* and *HY1* activity in the mutant might have decreased the production of the antioxidants CO and BV-IXα, resulting in increased cellular sensitivity to oxidants. Interestingly, the *AtHBP5* over-expression plants were less susceptible to MeJA treatment than the wild-type plants; although, the total haem concentration was not altered. Under these conditions, AtHBP5 did not influence the haem concentration but did afford the plant an additional protection against oxidative stress.

The findings in this report can be summarized and illustrated in a model (Fig. 6). Our data demonstrate that AtHBP5 and HY1 interact in *Arabidopsis* chloroplasts. Elimination of the *AtHBP5* transcript correlates with decreased *HY1* transcript and increased haem. Similarly, increased *AtHBP5* transcript correlates with slightly increased *HY1* transcript but with no change in the haem concentration. The mechanism of the resistance to oxidative stress may be through BV-IXα and CO, products of the HO reaction. BV-IXα has been shown to be an efficient scavenger of ROS and is thought to be the causative agent in the antioxidant response to Cd treatment (reviewed by Shekhawat and Verma, 2010). The fact that the *AtHBP5* transcript and protein abundance are inversely correlated with the accumulation of H_2O_2 is viewed as an important link between AtHBP5–HY1 interaction in chloroplasts and the ability to respond to oxidative stress in the plant.

Supplementary data

Supplementary data can be found at *JXB* online.

Supplementary Table S1. Primers used for PCR experiments described.

Supplementary Fig. S1. A phylogenetic tree of 62 higher plant SOUL/haem-binding proteins and sequence alignment.

Supplementary Fig. S2. BiFC analysis of AtHBP5 and HY1 binding *in vivo*.

Supplementary Fig. S3. Effect of light on hypocotyl elongation in the *athbp5* T-DNA mutant.

Acknowledgements

This work was supported in part by a Student Exchange Program between the Humboldt University Berlin and Tokyo University and by a grant from the Japan Student Services Organization (JASSO) during HJL's stay in Tokyo. We also thank Drs Olaf Czarnecki and Dieter Hackenberg (Plant Physiology, Institute of Biology, Humboldt University Berlin) for providing the vectors used in the protein–protein interaction studies.

References

Babusiak M, Man P, Sutak R, Petrak J, Vyoral D. 2005. Identification of heme binding protein complexes in murine erythroleukemic cells: study by a novel two-dimensional native separation–liquid chromatography and electrophoresis. *Proteomics* **5,** 340–350.

Balla J, Vercellotti GM, Nath K, Yachie A, Nagy E, Eaton JW, Balla G. 2003. Haem, haem oxygenase and ferritin in vascular endothelial cell injury. *Nephrology Dialysis Transplantation* **18,** Supplement 5, v8–12.

Chen X-Y, Ding X, Xu S, Wang R, Xuan W, Cao Z-Y, Chen J, Wu H-H, Ye M-B, Shen W-B. 2009. Endogenous hydrogen peroxide plays a positive role in the upregulation of heme oxygenase and acclimation to oxidative stress in wheat seedling leaves. *Journal of Integrative Plant Biology* **51,** 951–960.

Clough SJ, Bent AF. 1998. Floral dip: a simplified method for Agrobacterium-mediated transformation of *Arabidopsis thaliana*. *The Plant Journal* **16,** 735–743.

Davis SJ, Bhoo SH, Durski AM, Walker JM, Vierstra RD. 2001. The haem-oxygenase family required for phytochrome chromophore biosynthesis is necessary for proper photomorphogenesis in higher plants. *Plant Physiology* **126,** 656–669.

Davis SJ, Kurepa J, Vierstra RD. 1999. The *Arabidopsis thaliana* HY1 locus, required for phytochrome-chromophore biosynthesis, encodes a protein related to haem oxygenases. *Proceedings of the National Academy of Sciences, USA* **96,** 6541–6546.

Dias JS, Macedo AL, Ferreira GC, Peterson FC, Volkman BF, Goodfellow BJ. 2006. The first structure from the SOUL/HBP family of haem-binding proteins, murine P22HBP. *Journal of Biological Chemistry* **281,** 31553–31561.

Dóczi R, Brader G, Pettkó-Szandtner A, Rajh I, Djamei A, Pitzschke A, Teige M, Hirt H. 2007. The Arabidopsis mitogen-activated protein kinase kinase MKK3 is upstream of group C mitogen-activated protein kinases and participates in pathogen signaling. *The Plant Cell* **19,** 3266–3279.

Emanuelsson O, Brunak S, von Heijne G, Nielsen H. 2007. Locating proteins in the cell using TargetP, SignalP and related tools. *Nature Protocols* **2,** 953–971.

Emborg TJ, Walker JM, Noh B, Vierstra RD. 2006. Multiple heme oxygenase family members contribute to the biosynthesis of the phytochrome chromophore in Arabidopsis. *Plant Physiology* **140,** 856–868.

Espinas AN, Kobayashi K, Takahashi S, Mochizuki N, Masuda T. 2012. Evaluation of unbound free heme by differential extraction method. *Plant and Cell Physiology* **53,** 1344–1354.

Gisk B, Yasui Y, Kohchi T, Frankenberg–Dinkel N. 2010. Characterization of the haem oxygenase protein family in *Arabidopsis thaliana* reveals a diversity of functions. *Biochemical Journal* **425,** 425–434.

Gollhöfer J, Schläwicke C, Jungnick N, Schmidt W, Buckhout TJ. 2011. Members of a small family of nodulin-like genes are regulated under iron deficiency in roots of *Arabidopsis thaliana*. *Plant Physiology and Biochemistry* **49,** 557–564.

Gozzelino R, Jeney V, Soares MT. 2010. Mechanism of cell protection by heme oxygenase-1. *Annual Review of Pharmacology and Toxicology* **50,** 323–354.

Izawa T, Oikawa T, Tokutomi S, Okuno K, Shimamoto K. 2000. Phytochromes confer the photoperiodic control of flowering in rice (a short-day plant). *The Plant Journal* **22,** 391–399.

Jacob Blackmon B, Dailey TA, Lianchun X, Dailey HA. 2002. Characterization of a human and mouse tetrapyrrole-binding protein. *Archives of Biochemistry and Biophysics* **407,** 196–201.

Joyard J, Ferro M, Masselon C, Seigneurin-Berny D, Salvi D, Garin J, Rolland N. 2009. Chloroplast proteomics and the compartmentation of plastidial isoprenoid biosynthetic pathways. *Molecular Plant* **2,** 1154–1180.

Khan AA, Quigley JG. 2011. Control of intracellular heme levels: heme transporters and heme oxygenases. *Biochimica et Biophysica Acta 1813***,** 668–682.

Khanna R, Shen Y, Toledo-Ortiz G, Kikis EA, Johannesson H, Hwang Y-S, Quail PH. 2006. Functional profiling reveals that only a small number of phytochrome-regulated early-response genes in Arabidopsis are necessary for optimal deetiolation. *The Plant Cell* **18,** 2157–2171.

Kumar S, Bandyopadhyay U. 2005. Free heme toxicity and its detoxification systems in human. *Toxicology Letters* **157,** 175–188.

Lichtenthaler HK. 1987. Chlorophyll and carotenoids: pigments of photosynthetic biomembranes. *Methods in Enzymology* **148,** 349–382.

Marshall OJ. 2004. PerlPrimer: cross-platform, graphical primer design for standard, bisulphite and real-time PCR. *Bioinformatics* **20,** 2471–2472.

Melis A, Spangfort M, Andersson B. 1987. Light-absorption and electron-transport balance between photosystem II and photosystem I in spinach chloroplasts. *Photochemistry and Photobiology* **45,** 129–136.

Mills M, Payne SM. 1995. Genetics and regulation of heme iron transport in *Shigella dysenteriae* and detection of an analogous system in *Escherichia coli* O157:H7. *Journal of Bacteriology* **177,** 3004–3009.

Mochizuki N, Tanaka R, Grimm B, Masuda T, Moulin M, Smith AG, Tanaka A, Terry MJ. 2010. The cell biology of tetrapyrroles: a life and death struggle. *Trends in Plant Science* **15,** 488–498.

Muramoto T, Kohchi T, Yokota A, Hwang I, Goodman HM. 1999. The Arabidopsis photomorphogenic mutant *hy1* is deficient in phytochrome chromophore biosynthesis as a result of a mutation in a plastid haem oxygenase. *The Plant Cell* **11,** 335–348.

Noriega GO, Balestrasse KB, Batlle A, Tomaro ML. 2004. Heme oxygenase exerts a protective role against oxidative stress in soybean leaves. *Biochemical and Biophysical Research Communications* **323,** 1003–1008.

Poss KD, Tonegawa S. 1997. Reduced stress defense in haem oxygenase 1-deficient cells. *Proceedings of the National Academy of Sciences*, *USA.* **94,** 10925–10930.

Roper JM, Smith AG. 1997. Molecular localisation of ferrochelatase in higher plant chloroplasts. *European Journal of Biochemistry* **246,** 32–37.

Santa–Cruz DM, Pacienza NA, Polizio AH, Balestrasse KB, Tomaro ML, Yannarelli GG. 2010. Nitric oxide synthase-like dependent NO production enhances haem oxygenase up-regulation in ultraviolet-B-irradiated soybean plants. *Phytochemistry* **71,** 1700–1707.

Sato E, Sagami I, Uchida T, Sato A, Kitagawa T, Igarashi J, Shimizu T. 2004. SOUL in mouse eyes is a new hexameric heme-binding protein with characteristic optical absorption, resonance Raman spectral, and heme-binding properties. *Biochemistry* **43,** 14189–14198.

Shekhawat GS, Verma K. 2010. Haem oxygenase (HO): an overlooked enzyme of plant metabolism and defence. *Journal of Experimental Botany* **61,** 2255–2270.

Takahashi S, Ogawa T, Inoue K, Masuda T. 2008. Characterization of cytosolic tetrapyrrole-binding proteins in *Arabidopsis thaliana*. *Photochemistry and Photobiology Sciences* **7,** 1216–1224.

Taketani S, Adachi Y, Kohno H, Ikehara S, Tokunaga R, Ishii T. 1998. Molecular characterization of a newly identified heme-binding protein induced during differentiation of urine erythroleukemia cells. *Journal of Biological Chemistry* **273,** 31388–31394.

Tamura K, Peterson D, Peterson N, Stecher G, Nei M, Kumar S. 2011. MEGA5: molecular evolutionary genetics analysis using maximum likelihood, evolutionary distance, and maximum parsimony methods. *Molecular Biology and Evolution* **28,** 2731–2739.

Terry MJ, Linley PJ, Kohchi T. 2002. Making light of it: the role of plant haem oxygenases in phytochrome chromophore synthesis. *Biochemical Society Transactions* **30,** 604–609.

True AL, Olive M, Boehm M, *et al.* 2007. Heme oxygenase-1 deficiency accelerates formation of arterial thrombosis through oxidative damage to the endothelium, which is rescued by inhaled carbon monoxide. *Circulation Research* **101,** 893–901.

Walter M, Chaban C, Schütze K, *et al.* 2004. Visualization of protein interactions in living plant cells using bimolecular fluorescence complementation. *The Plant Journal* **40,** 428–438.

Wanker EE, Rovira C, Scherzinger E, Hasenbank R, Wälter S, Tait D, Colicelli J, Lehrach H. 1997. HIP-I: a huntingtin interacting protein isolated by the yeast two-hybrid system. *Human Molecular Genetics* **6,** 487–495.

Wu M, Huang J, Xu S, Ling T, Xie Y, Shen W. 2011. Haem oxygenase delays programmed cell death in wheat aleurone layers by modulation of hydrogen peroxide metabolism. *Journal of. Experimental Botany* **62,** 235–248.

Yannarelli GG, Noriega GO, Batlle A, Tomaro ML. 2006. Heme oxygenase up-regulation in ultraviolet-B irradiated soybean plants involves reactive oxygen species. *Planta* **224,** 1154–1162.

Zhang L, Xing D. 2008. Methyl jasmonate induces production of reactive oxygen species and alterations in mitochondrial dynamics that precede photosynthetic dysfunction and subsequent cell death. *Plant and Cell Physiology* **49,** 1092–1111.

Zhou B, Wang J, Guo Z, Tan H, Zhu X. 2006. A simple colorimetric method for determination of hydrogen peroxide in plant tissues. *Plant Growth Regulation* **49,** 113–118.

Zybailov B, Rutschow H, Friso G, Rudella A, Emanuelsson O, Sun Q, van Wijk KJ. 2008. Sorting signals, N-terminal modifications and abundance of the chloroplast proteome. *PLoS ONE* **3,** e1994.

Zylka MJ, **Reppert SM.** 1999. Discovery of a putative haem-binding protein family (SOUL/HBP) by two-tissue suppression subtractive hybridization and database searches. *Brain Research Molecular Brain Research* **74,** 175–181.